FUNCTIONALIZATION OF GRAPHENE NANOPLATELETS WITH AN ELASTOMER CTBN AND THE EFFECT ON THE VINYL ESTER NANOCOMPOSITES

S. G. Ji[1], D. Kim[1], D. Cho[1]*, I. Do[2], H. Fukushima[2], L. T. Drzal[2]
[1] Department of Polymer Science and Engineering, Kumoh National Institute of Technology, Gumi, Gyeongbuk 730-701, Korea
[2] Composite Materials and Structures Center, Michigan State University, East Lansing, MI 48824, USA
* Corresponding author(dcho@kumoh.ac.kr)

Keywords: *Graphene Nanoplatelets, Functionalization, CTBN, Vinyl Ester Nanocomposites*

1. Introduction

Polymer nanocomposites reinforced with carbon nanotube, graphene or graphite nanoparticles of very low weight or volume fraction have attracted increasingly due to their peculiar and fascinating properties as well as their unique academic and industrial applications. Recently, exfoliated graphite or graphene nanoplatelets have been paid attractive attention as promising carbon nanoparticles for polymer nanocomposites [1]. The incorporation of graphite nanoparticles such as exfoliated graphite nanoplatelets or graphene sheets arranged in nanometer scale with a high aspect ratio and/or an extremely large surface area into polymers may improve their mechanical performances significantly. The properties of polymer nanocomposites depend greatly on the chemistry of polymer matrix, the nature and dispersion of nanofillers, polymer-nanofiller interfaces, and the preparation method.

Vinyl ester (VE) resins have been widely used as matrix in carbon fiber composites. They have combined characteristics of epoxy and unsaturated polyester resins. They have not only excellent resistance to water, organic solvents and corrosion but also excellent processibility. VE resins can be cured much like unsaturated polyesters, based on the unsaturated chains, and are, therefore, easier to cure than epoxies. As VE resins are filled with xGnP at various contents, they may exhibit lower impact resistance, compared to the unfilled counterpart [2]. The mechanical properties of a carbon/VE composite are currently less than those of a carbon/epoxy counterpart, due partly to its low interfacial adhesion between carbon fibers and VE matrix [3].

It has been well known that elastomeric molecules and particles can be added to increase the toughness of thermosetting polymers. However a significant amount of elastomer may be needed to exhibit the toughening effect and may cause a reduction of the mechanical properties [4-6].

Consequently, the primary objectives of the present study are to functionalize exfoliated graphene nanoplatelets (xGnP) with a liquid rubber carboxyl-terminated poly(butadiene-*co*-acrylonitrile) (CTBN) by grafting and to fabricate successful xGnP/VE nanocomposites. The ultimate objectives are to improve the impact toughness of the xGnP/VE nanocomposite as well as VE, to enhance their mechanical properties and also to reduce the electrical resistivity.

2. Experimental

2.1 Materials

Graphite intercalation compound (GIC 3772) was supplied from Asubury Graphite Mills, Inc., NJ, USA. It was used as starting material for preparing exfoliated graphene nanoplatelets. Fuming nitric acid, sodium chlorate, thionyl chloride, pyridine, *N*,*N*-dimethyl formamide, and liquid-state rubber CTBN (Hypro™ CTBN 1300x13, Hycar, USA) were used in this study (Fig. 1). Vinyl ester resin (DERAKANE 411-350), supplied from Ashland Specialty Chemical, Co., OH, USA, was used as received (Fig. 1). Methyl ethyl ketone peroxide as initiator and cobalt naphthenate as accelerator were used for curing VE.

2.2 Preparation of CTBN-functionalized xGnP

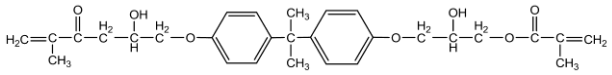

(A)

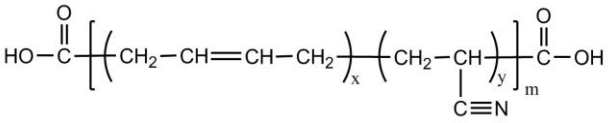

(B)

Fig. 1. The molecular structures of vinyl ester resin (A) and carboxyl-terminated poly(butadiene-*co*-acrylonitrile) (B).

Exfoliated graphene nanoplatelets prepared from the intercalated graphite compound were oxidized by the Brodie's method and then neutralized over and over again until it reached near pH7, producing graphite oxides (GO). Then it was vigorously stirred with thionyl chloride and pyridine at 70℃. The acyl chloride-functionalized xGnP was immediately reacted with *N*,*N*-dimethyl formamide (DMF) and CTBN at a 100℃. The excess solution was washed out with acetone ten times and then the acetone was removed at 45℃ in a vacuum oven. Finally, CTBN-functionalized xGnP was obtained.

2.3 Fabrication of VE, xGnP/VE and CTBN-functionalized xGnP/VE Nanocomposites

The mixture of neat VE resin, initiator and accelerator was poured into the Teflon™ (Dupont) mold. The xGnP and CTBN-functionalized xGnP contents in the VE nanocomposites were 1, 3 and 5 wt.%, respectively. Each mold was heated with multiple steps up to 120℃ in a vacuum oven for complete curing of VE.

2.4 Characterization of xGnP

Attenuated total reflection-Fourier transform infrared (ATR-FTIR) (Jasco 300E spectrophotometer, Japan) spectroscopy was performed to analyze surface functional groups of the xGnP and carboxylated xGnP. All of the samples were of powder and the range of wavenumber was 4000 to 500 cm^{-1}. The total scanned number was 32.
In order to assess the surface functional groups, X-ray photoelectron (XPS) spectroscopy was performed using a Thermo Fisher Scientific (UK) Multilab-2000 XPS spectrometer. The X-ray source was Al-Kα radiation. The lens mode and energy step size were LAXPS and 0.1eV, respectively. The photoelectron peaks (narrow scan spectra) were fitted by Fityk program (ver. 0.9.4) made by M. Wojdyr and the peaks intensity was obtained from the Gaussian relation.
Raman spectroscopic measurements were carried out using a Micro Raman spectrometer (Renishaw, system 100, UK) in the range of 3000 to 500 cm-1.
The thermal stability of xGnP, carboxylated xGnP and CTBN-functionalized xGnP was measured using a thermogravimetric analyzer (TA Instruments, Q500) in nitrogen atmosphere. The heating rate was 5℃/min.

2.5 Characterization of Nanocomposites

The impacts tests for VE control, xGnP/VE and CTBN-funtionalized xGnP/VE nanocomposites were performed at ambient temperature with an 18.54 N hammer weight and with 21.6 J impact energy according to ASTM D256 using an Izod-type impact tester (Tinius Olsen Model-892, USA) to examine the change of impact strength depending on the xGnP nanoparticles incorporated. All of the samples were unnotched and the dimensions were 62 mm x 10.2 mm x 3.2 mm. The average impact strength of each sample was obtained from successful ten specimens.
The surface resistivity of VE control, xGnP/VE and CTBN-funtionalized xGnP/VE nanocomposites was measured using 4-point-probe surface resistivity apparatus (AiT: CMT-SR1000N) at room temperature. The sample dimensions of 150 mm x 12 mm x 3 mm were obtained from the middle portion of original specimen bars by grinding and the surface resistivity was measured along the length direction (15 mm). The average value of surface resistivity was obtained from successful ten specimens.

3. Results and Discussion

ATR-FTIR spectroscopy is useful to study surface functional groups of organic materials. Fig. 2 shows the ATR-FTIR spectra of xGnP and carboxylated xGnP (24 h acid treatment). Before acid treatment, the characteristic absorption peaks were not detected from the xGnP because it has no functional groups on the surfaces. The xGnP is mostly composed of carbon atoms and a tiny

amount of residual unreacted intercalant may also be existed. As can be seen, the spectrum from carboxylated xGnP exhibited a broad peak around 3442 cm^{-1}, which was derived from O-H stretching vibration of carboxyl and hydroxyl groups. The other characteristic peaks appeared at 1737 cm^{-1} and 1616 cm^{-1} were due to C=O stretching vibration of carboxyl groups and to C-O stretching vibration of epoxide groups, respectively. The result indicated that a lot of carboxyl groups were formed on the xGnP surfaces by the acid treatment.

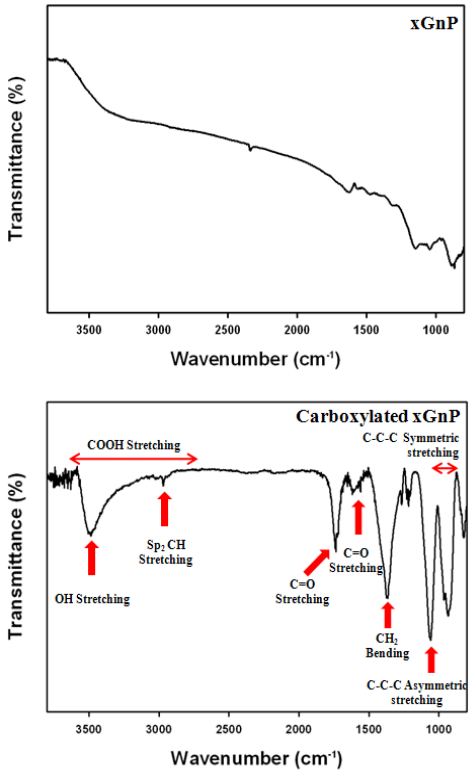

Fig. 2. ATR-FTIR spectra of xGnP and carboxylated xGnP.

Generally, XPS offers qualitative and quantitative chemical information and it is a powerful tool to analyze surface chemical groups of materials. Table 1 summarizes the atomic compositions of xGnP, carboxylated xGnP and CTBN-functionalized xGnP obtained from the XPS wide scan result. The carbon and oxygen contents were 97.52%, 2.48% for xGnP and 75.18% and 24.82% for carboxylated xGnP, respectively. In the carboxylated xGnP, the carbon contents were largely decreased whereas the oxygen contents were significantly increased. Therefore it can be said that carboxylated xGnP includes the oxygen-containing groups like COOH, C-OH, C-O, etc. Carbon, oxygen and nitrogen atoms were also detected in the CTBN-functionalized xGnP. The amounts of carbon, oxygen and nitrogen atoms of CTBN-functionalized xGnP were 88.04%, 10.28% and 1.68%, respectively. In the CTBN-functionalized xGnP, the presence of the nitrogen atom demonstrated the existence of the CTBN grafted on the surfaces of xGnP.

Table 1. Atomic compositions of xGnP, carboxylated xGnP and CTBN-functionalized-xGnP analyzed from XPS

Material	C (%)	O (%)	N (%)
xGnP	97.52	2.48	0
Carboxylated xGnP	75.18	24.82	0
CTBN functionalized-xGnP	88.04	10.28	1.68

Fig. 3 displays the thermal stability of xGnP, carboxylated xGnP and CTBN-functionalized xGnP. The xGnP exhibited excellent thermal stability up to 800℃. There was a slight weight loss occurred below 100℃ in the carboxylated xGnP because of the evaporation of absorbed water molecules. The drastic weight loss of carboxylated xGnP occurred near 270℃ may be due to the thermal degradation of the functional groups containing oxygen atoms. This result also reflected that the level of the functional groups such as hydroxyl, epoxide and carboxyl groups attached by the acid treatment to the xGnP. The CTBN-functionalized xGnP was relatively more stable

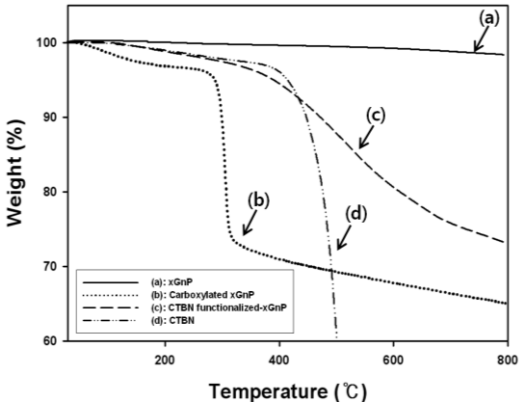

Fig. 3. TGA curves of (a) xGnP, (b) carboxylated xGnP, and (c) CTBN functionalized xGnP.

than the carboxylated xGnP. This can be explained by the thermal degradation curve of CTBN chemically bonded to xGnP.

Fig. 4 shows Raman spectra for xGnP, carboxylated xGnP and CTBN-functionalized xGnP. The first peak (D band) at 1357 cm^{-1} is ascribed to the disorder or defect structure of xGnP and carboxylated xGnP. The second peak (G band) at 1591 cm^{-1} is due to the well-ordered structure. The intensity ratio (I_D/I_G) of the xGnP was about 0.12. However the ratio of carboxylated xGnP was 0.89. The third peak (2D band) at 2700 cm^{-1} corresponds to the overtone of the D band which is sensitive to the number of graphene layers. The 2D band was decreased, indicating that functional groups such as COOH, C-OH and C-O groups were attached to xGnP by acid treatment. However in the CTBN-functionalized xGnP, the I_D/I_G ratio was decreased to 0.55 again and the G band and 2D band were shifted back to the position of the G band in the xGnP.

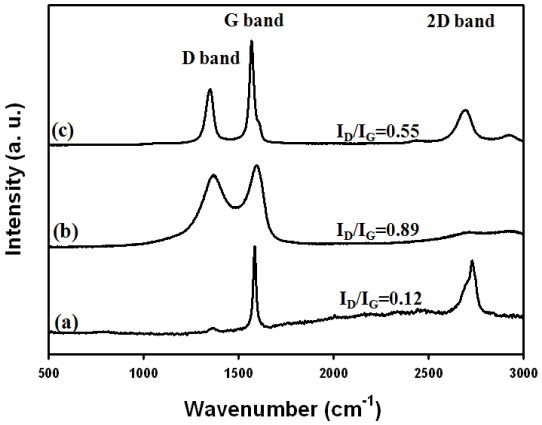

Fig. 4. Raman spectra of (a) xGnP, (b) carboxylated xGnP and (c) CTBN-functionalized xGnP.

Based on the analytical results (FTIR, XPS, micro-Raman, and TGA), a reaction scheme with a series of experimental steps for grafting of CTBN to xGnP has been proposed, as illustrated in Fig. 5. In the first step, xGnP was well oxidized under the optimal acid treatment condition by the Brodie's method and a plenty of oxygen-containing functional groups, especially carboxyl groups, were attached to the xGnP, resulting in carboxylated xGnP. In the second step, acyl chloride groups with an extremely high reactivity generated by the reaction with thionyl chloride were successfully introduced to the carboxylated xGnP. In the final step, acyl chloride-functionalized xGnP was reacted with carboxyl groups of CTBN by esterification. Therefore it has been concluded that the elastomeric CTBN chains were successfully grafted and covalently bonded to xGnP, as demonstrated by multiple analytical evidences.

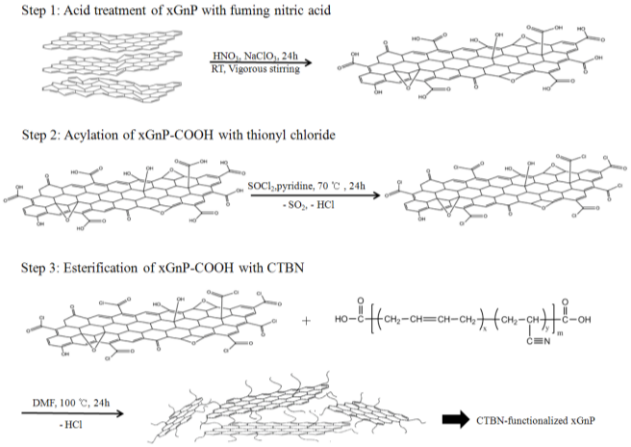

Fig. 5. Proposed reaction scheme from xGnP to CTBN-functionalized xGnP through acylation and esterification of carboxylated xGnP.

Fig. 6 exhibits the Izod impact strength of the VE, VE/xGnP and VE/CTBN-functionalized xGnP nanocomposites with different xGnP contents. The impact strength of VE resin was 77.62 J/m. However the impact strength of neat VE resin was decreased about 25% by incorporating untreated 1 wt.% xGnP. At the 3 wt.% xGnP, the impact strength of xGnP/VE nanocomposites was improved about 20%, compared to neat VE resin. In the 5 wt% xGnP, the impact strength was similar to the 3 wt.% xGnP. The impact strength of VE resin was greatly increased about 65% from 77.62 J/m to 124.18 J/m by incorporating only 1 wt% CTBN-functionalized xGnP and further markedly increased with increasing CTBN-functionalized xGnP. It was noted that the impact strength was significantly improved with increasing CTBN-functionalized xGnP contents, exhibiting 238% improvement compared with neat VE and also 178% improvement, compared with pristine xGnP/VE nanocomposite, particularly at a 5 wt% loading of CTBN-functionalized xGnP.

Fig. 7 shows the effect of xGnP and CTBN-functionalized xGnP with different contents on the

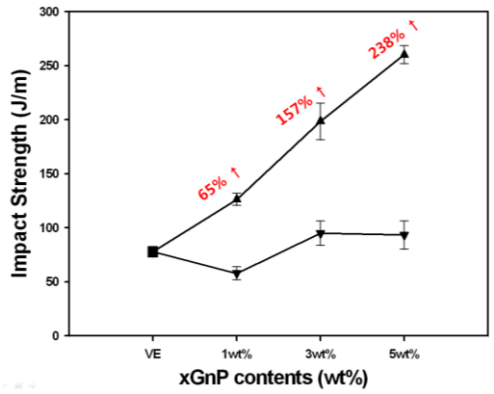

Fig. 6. Variation of the impact strengths of neat VE, xGnP/VE and CTBN-functionalized xGnP/VE nanocomposites with different xGnP contents.

surface resistivity of VE. The surface resistivity of VE was about 1011 (Ω/sq). The surface resistivity was significantly changed with the incorporation of xGnP. At 1 wt% xGnP, the surface resistivity was similar to the VE. At 3 wt% xGnP, there was a significant decrease of electrical resistivity measured. This stepwise change in the surface electrical resistivity was a result of the formation of an interconnected structure of xGnP and can be regarded as electrical percolation threshold. It means that many electrons are permitted to move around the nanocomposites by the creation of an inter-connecting conductive pathway. Above 3 wt% xGnP, the surface resistivity was significantly decreased. This result also supports that the CTBN molecules, which are not electrically conductive at all, were successfully grafted to the xGnP and were well dispersed in the VE matrix of the nanocomposite.

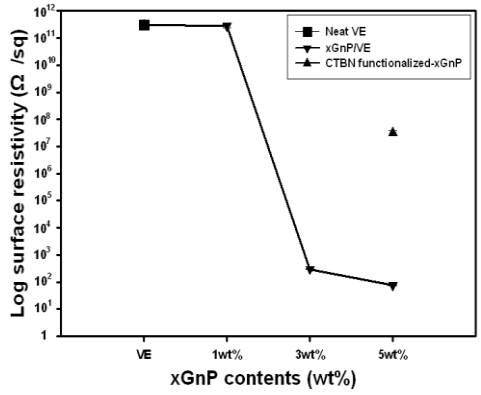

Fig. 7. Surface resistivity of neat VE, xGnP/VE and CTBN-functionalized xGnP/VE nanocomposites fabricated with different xGnP contents.

At 5 wt% CTBN-functionalized xGnP (filled triangle), the surface resistivity was observed and the value was intermediate between xGnP(3 wt%)/VE and xGnP(5 wt%)/VE nanocomposites. At CTBN-functionalized xGnP contents less than 5 wt%, the resistivity was extremely high so that the measurements were not successfully performed, reflecting totally nonconductive nature of the nanocomposite with CTBN-grafted xGnP particles.

4. Conclusions

It was demonstrated by multiple analytical studies that exfoliated graphene nanoplatelets were oxidized by the Brodie's method and CTBN was successfully grafted to the xGnP through the acid treatment, acylation and esterification. It has been also revealed that the incorporation of CTBN-functionalized xGnP into neat vinyl ester resin markedly improves the impact strength of xGnP/VE nanocomposites depending on the CTBN-functionalized xGnP content. The electrical resistivity of neat resin and the xGnP/VE nanocomposite was greatly reduced at above 1 wt% xGnP content, elucidating the toughening effect of neat VE resin and un-modified xGnP/VE nanocomposite by CTBN-functionalized xGnP particles of a very small amount incorporated therein. The CTBN-functionalized xGnP(5 wt%)/VE nanocomposite exhibited the intermediate electrical resistivity of 10^7-10^8 Ω/sq due to the combination of nonconductive CTBN molecules and dispersed conductive xGnP particles in the nanocomposite.

References

[1] S. Tjong "Structural and mechanical properties of polymer nanocomposites". *Materials Science and Engineering*, Vol 53, No. 3-4, 73-197, 2006.

[2] W. Liu, I. Do, H. Fukushima, and L. T. Drzal, "The effect of exfoliated graphite nanoplatelet size on the mechanical and electrical properties of vinyl ester nanocomposites", *Proceedings of SAMPE*, 2008.

[3] M. A. F. Robertson, M. B. Bump, K. E. Vergese, S. R. McCartney, J. J. Lesko, J. S. Riffle, I. C. Kim, and T. H. Yoon, "Designed interface regions in carbon fiber reinforced vinyl ester matrix composites", *Journal of Adhesion*, Vol 71, 395-416, 1999.

[4] T. Wang and C. Tseng "Polymeric carbon nanocomposits from multiwalled carbon nanotubes functionalized with segmented polyurethane". *Journal of Applied Polymer Science*, Vol 105, 1642-

1630, 2007.
[5] X. Chen, M. Lin, W. Zhong and Z. Chen "Functionalized multi-walled carbon nanotubes prepared by in situ polycondensation of polyurethane". *Macromolecular Chemistry and Physics*, Vol 208, 964-972, 2007.
[6] X. Chen, J. Wang, J. Zou, X. Wu and F. Xue, "Mechanical and thermal properties of functionalized multiwalled carbon nanotubes and multiwalled carbon nanotube-polyurethane composites". *Journal of Applied Polymer Science*, Vol 114, 3407-3413, 2009.